ISSN: 2472-3703 DOI: 10.6911/WSRJ.202304_9(4).0012

Carbon Fiber Cloth Reinforced Steel Tube Concrete Composite Structure

Songbiao Li

Department of Civil Engineering, Henan Polytechnic University, Jiaozuo 454003, China

Abstract

Modern building structure has high requirements for the mechanical properties of the load-bearing column, combined with the development of material mechanics, the composite reinforcement of the new steel tube concrete composite structure is proposed, which has the advantages of convenient construction and low cost. The finite element analysis software Abaqus was used to simulate and analyze the mechanical properties of such new composite steel-concrete structures after being reinforced with carbon fiber cloth, and the control variables were the arrangement height, number of layers and arrangement direction of fiber cloth, and different types of combined structures. The result is that the ultimate bearing capacity of ordinary steel tube concrete specimens is increased by about 3% under the single-layer arrangement. Among them, the ultimate bearing capacity error between the maximum arrangement of the three layers and the unarranged specimen is 8%, and the conclusion obtained in this paper is that the setting of carbon fiber cloth reinforcement can significantly improve the mechanical properties of the specimen.

Keywords

Abaqus; Nonlinear; CFST; CFRP.

1. INTRODUCTION

With the development of building structure, the mechanical properties of the bearing column requirements are high, in order to meet the large span, the tall structure Some scholars have proposed that the use of steel tube concrete column combination structure can make up for the poor ductility of concrete [1], and can prevent steel compression buckling, this type of structure has been widely used in practical engineering after a long period of development and research [2], the development of composite materials, the reinforcement of such columns, provides greater convenience [3]

2. FINITE ELEMENT ANALYSIS DESIGN

2.1. Test piece size

Take the A1, A2, A3, A4, A5, A6 specimens and their model sizes according to the settings in Table 1, and the model and specific carbon fiber settings of typical specimens are shown in Figure 1. Among them, the height distribution of carbon fiber cloth is taken$h/4$； $h/2$； h。 h is the height of the specimen. The number of layers is divided into three types, and the arrangement position is centered symmetrically on the height of the specimen.

ISSN: 2472-3703 DOI: 10.6911/WSRJ.202304_9(4).0012

Table 1. Model dimensions

numbering	$\frac{(h \times t)}{mm}$	$\frac{(h_s \times t_s)}{mm}$	$\frac{r_s \times l_s \times b_s}{mm}$	n
A1	150 x 1.9	—	—	0
A2	150 x 1.9	27 x 1.9	—	0
A3	150 x 1.9	—	2.5 x 150 x 120	4
A4	150 x 1.9	27x1.9	2 x 150 x 120	4
A5	150 x 1.9	27 x 1.9	3 x 150 x 120	4
A6	150 x 1.9	27 x 1.9	2.5 x 150 x 120	4

Table: $h$is the section width of the steel pipe, $t$is the thickness of the steel pipe wall, h_s is the cross-sectional length of the stiffener

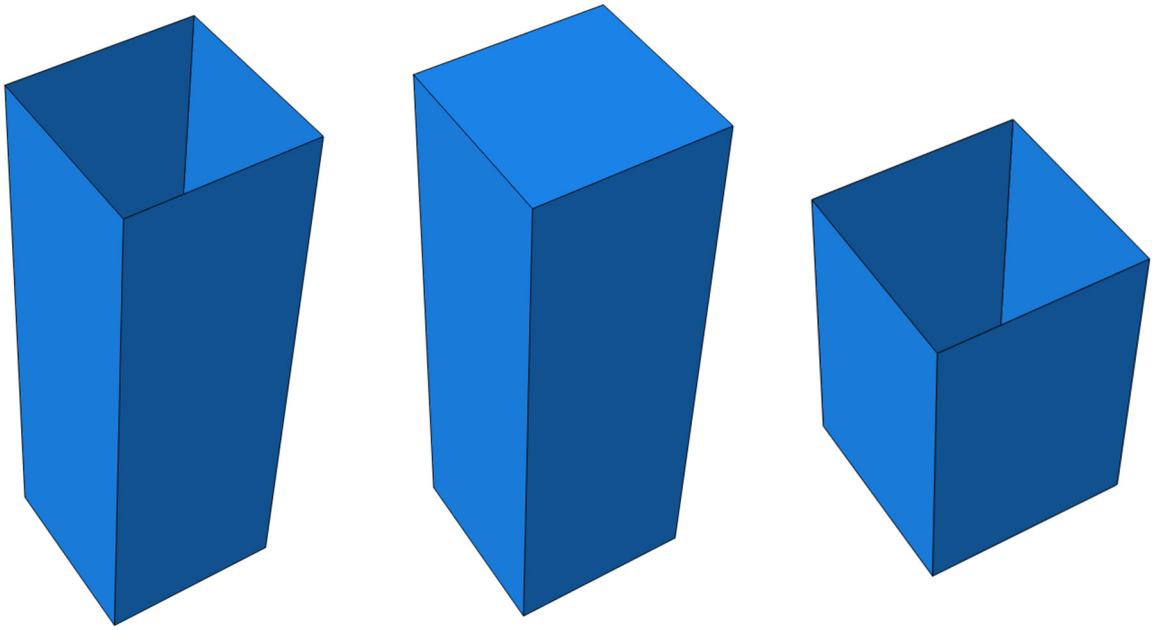

(a) Steel tube (b) Concrete (c) Carbon fiber cloth

Figure 1. Model assembly drawing

2.2. Material properties

2.2.1 Steel

The steel adopts the secondary plastic flow model, which is low carbon steel, for which the stress-strain curve of the steel is divided into five stages; The first is the elastic phase with less stress; As the stress increases, the steel enters the elastoplastic stage; Subsequently, it enters the plastic stage, and the material enters the strengthening section as strain accumulates; Finally, the secondary plastic flow stage is entered to reach the maximum tensile strength. f_y, f_p, f_u They are the proportion limit, yield strength and tensile strength limit of steel[4]. The steel yields to meet the Von-mises yield criterion.

ISSN: 2472-3703 DOI: 10.6911/WSRJ.202304_9(4).0012

$$\sigma = \begin{cases} E_S\varepsilon & (\varepsilon \le \varepsilon_e) \\ f_p + \dfrac{\varepsilon - \varepsilon_e}{\varepsilon_{e1} - \varepsilon_e}(f_y - f_p) & (\varepsilon_e < \varepsilon \le \varepsilon_{e1}) \\ f_y & (\varepsilon_{e1} < \varepsilon \le \varepsilon_{e2}) \\ f_y + \dfrac{\varepsilon - \varepsilon_{e2}}{\varepsilon_{e2} - \varepsilon_{e1}}(f_u - f_y) & (\epsilon_{e2} < \varepsilon < \varepsilon_{e3}) \\ f_u & (\varepsilon > \varepsilon_{e3}) \end{cases} \quad (1)$$

Formula: $\varepsilon_e = \frac{0.8f_y}{E_s}$, $\varepsilon_{e1} = 1.5\varepsilon_e$, $\varepsilon_{e2} = 10\varepsilon_{e1}, \varepsilon_{e3} = 100\varepsilon_{e1}$

2.2.1 Concrete

When steel pipe concrete is subjected to axial pressure, the Poisson's ratio and material properties of steel pipe and concrete are different, and the lateral deformation is not coordinated during the bearing process, resulting in interaction between steel pipe and concrete. The steel pipe has a certain hydrostatic pressure on the radial and circumferential direction of the core concrete; After summarizing a large number of test data of steel tube concrete, Han Linhai proposed a concrete compression constituent suitable for square section steel tube concrete columns, which is widely used in the numerical analysis of steel tube concrete, including axial pressure and bias [5].

$$y = \begin{cases} 2x - x^2 & x \le 1 \\ \dfrac{x}{\beta_o(x-1)^\eta + x} & x > 1 \end{cases} \quad (2)$$

Formula: $x = \frac{\varepsilon}{\varepsilon_o}$, $y = \frac{\sigma}{\sigma_o}$

$\sigma_o = f_c'$, $\varepsilon_o = \varepsilon_c + 800\xi^{0.2} \times 10^{-6}$, $\varepsilon_c = (1300 + 12.5 \times f_c') \times 10^{-6}$

$\eta = 1.6 + \frac{1.5}{x}$, $\beta_o = \frac{(f_c')^{0.1}}{1.2(1+\xi)^{0.5}}$, $\xi = \frac{A_s \times F_s}{A_c \times F_c}$

The damage to concrete was calculated using the CDP figurine method

2.2.3 CFRP constitution

The force along the fiber length direction is the main force mode, and the force of the remaining methods is calculated according to the summary of a large number of literature, and the strength of the remaining directions is 0.001MPa in the length direction. For the constitutive relation in the direction of length, see Equation (3)

$$F_{cft} = E_{cf} * \varepsilon_{ft} \quad (3)$$

Formula: F_{cft} is the fiber length pulling force, E_{cf} is the elastic modulus in the length direction, ε_{ft} is a tensile strain function.

2.2.4 Interaction and boundary conditions

The friction coefficient of 0.6 is adopted for the tangential properties of steel pipe and concrete, in order to avoid stress concentration at the junction, the bonding strength between fiber cloth and steel pipe or concrete is large in the comprehensive literature, and the Tie constraint is usually considered in the finite element. The two endpoints of the specimen are contacted with the loading plate by coupling method, and loaded by applying forced displacement.

ISSN: 2472-3703 DOI: 10.6911/WSRJ.202304_9(4).0012

3. ANALYSIS OF FINITE ELEMENT SIMULATION RESULTS

3.1. Single-layer paste analysis

Taking typical specimens A1, A2 and A4 as the analysis objects, the influence of fibers on the mechanical properties of specimens at three heights was considered. Table 1 shows the ultimate bearing capacity and ductility of typical specimens.

Table 2. Mechanical properties

NUMBER	N_Y	DI_Y	$N_{H112.5}$	$DI_{H112.5}$	N_{H225}	DI_{H225}	N_{H450}	DI_{H450}
A1	1020	2.80	1038.18	2.83	1053.42	2.85	1074.99	2.92
A2	1149	3.08	1166.41	3.13	1171.23	3.20	1175.12	3.21
A4	1212	3.51	1224.99	3.56	1231.93	3.59	1236.2	3.62

It can be seen from Table 1 that when pasting carbon fiber cloth in a single layer, the ultimate bearing capacity and ductility of the specimen are very small when the height of the fiber cloth is small, for example, when the fiber height of A1, A2 and A4 specimens is 112.5, the ultimate bearing capacity is increased by 1.37%, 1.51%, 7%, respectively, and the ductility improvement is basically ignored, which indicates that only a single layer of small-range carbon fiber cloth is used to reinforce the middle of the specimen under axial pressure load, and the ultimate bearing capacity of the specimen is increased small, and the peak point is not backward.

The ultimate bearing capacity and ductility of A1 specimen fiber cloth height of 450mm are increased by 2% and 3% respectively compared with 112.5mm, and it can be seen from Figure 3 that the peak bearing capacity has a backward trend. Both A2 and A4 specimens have this characteristic and will not be repeated.

A2 compared with A1 in the 450mm reinforcement of its ultimate bearing capacity difference proportion is less than the difference without setting carbon fiber cloth, which is related to the restraining force provided by carbon fiber cloth to reduce the deformation of the specimen, when the steel pipe wall of A1 specimen is far from the corner of the anti-lateral shift stiffness attenuation is large, easy to produce local buckling failure resulting in the inability to fully play the role of steel, the addition of fiber cloth to a certain extent improves the anti-lateral rigidity of the weak position of the steel pipe wall, for A2 specimens due to the setting of ribs, The anti-lateral rigidity of the steel pipe wall is greatly improved, and when the carbon fiber cloth is pasted in a single layer, the lateral deformation of the specimen is less affected, which is the main reason for the decrease in the bearing capacity difference.

When the fiber cloth of A2 specimen is pasted with one layer, the ultimate bearing capacity and the specimen without fiber cloth are increased by 1.93% and 2.27% respectively when the height of 225mm and 450mm is pasted.

The ultimate bearing capacity of 225mm and 450mm height of A4 specimens is increased by 1.64% and 1.98% respectively compared with the unset parts under the condition of single-layer pasted fiber cloth, and Figure 2 shows the curve of the ultimate bearing capacity increase curve of A1, A2 and A4 specimens under single-layer arrangement.

ISSN: 2472-3703 DOI: 10.6911/WSRJ.202304_9(4).0012

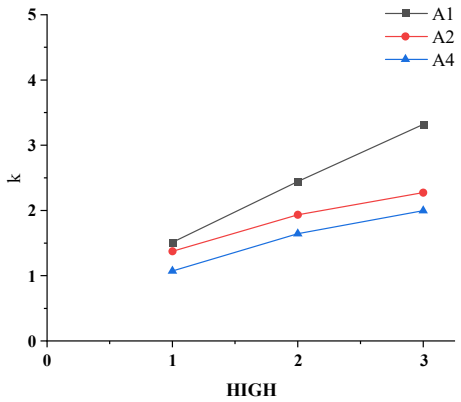

Figure 2. Increase the scale

From Figure 2 and the above analysis, it can be seen that the ultimate bearing capacity increase value under the single layer of fiber cloth is small, and A1 compared with the rest of the parts, with the increase of the height of the fiber cloth, the proportion of ultimate bearing capacity increase increases, and the curve corresponds to the factors given in the above analysis.

3.2. Load-displacement curve analysis of specimens

Figure 3 shows the load displacement curves of typical specimens A1, A2 and A4 considering different reinforcement heights

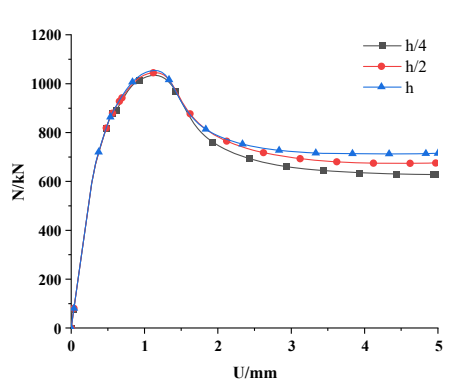

(a)A1

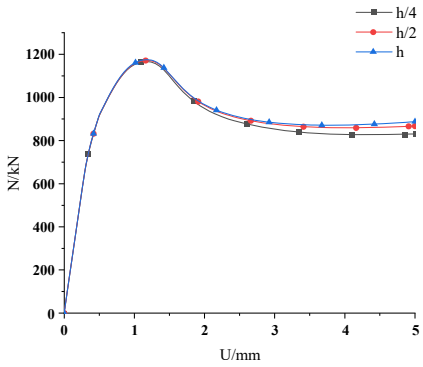

(b)A2

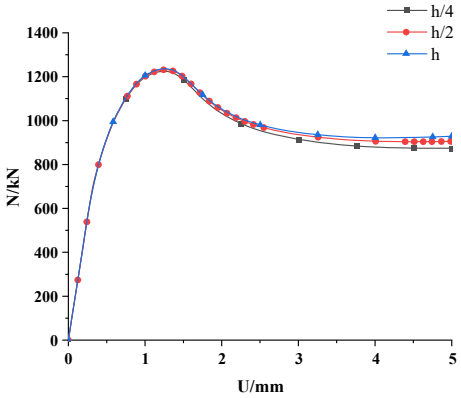

(C)A4

Figure 3. Load displacement curve of a typical specimen

ISSN: 2472-3703 DOI: 10.6911/WSRJ.202304_9(4).0012

It can be seen from the figure that the load-line of the specimen includes the rising and falling sections, and the early curves of each specimen almost coincide, because the specimen is in a small deformation state, and the restraining effect of the fiber cloth on the specimen is not obvious; As the load increases to $0.8N_{xwb}$, the load displacement curve of the fiber cloth is pasted at different heights, and the load displacement curve begins to appear significantly slitting, which is more obvious for A1 specimens. As the load continues to increase, compared with A2 and A4, the peak load shifts more significantly with the increase of the adhesive height. Each specimen in the descending section is manifested as that the larger the pasting height, the smoother the curve falls.

3.3. Comparison of the number of different paste layers

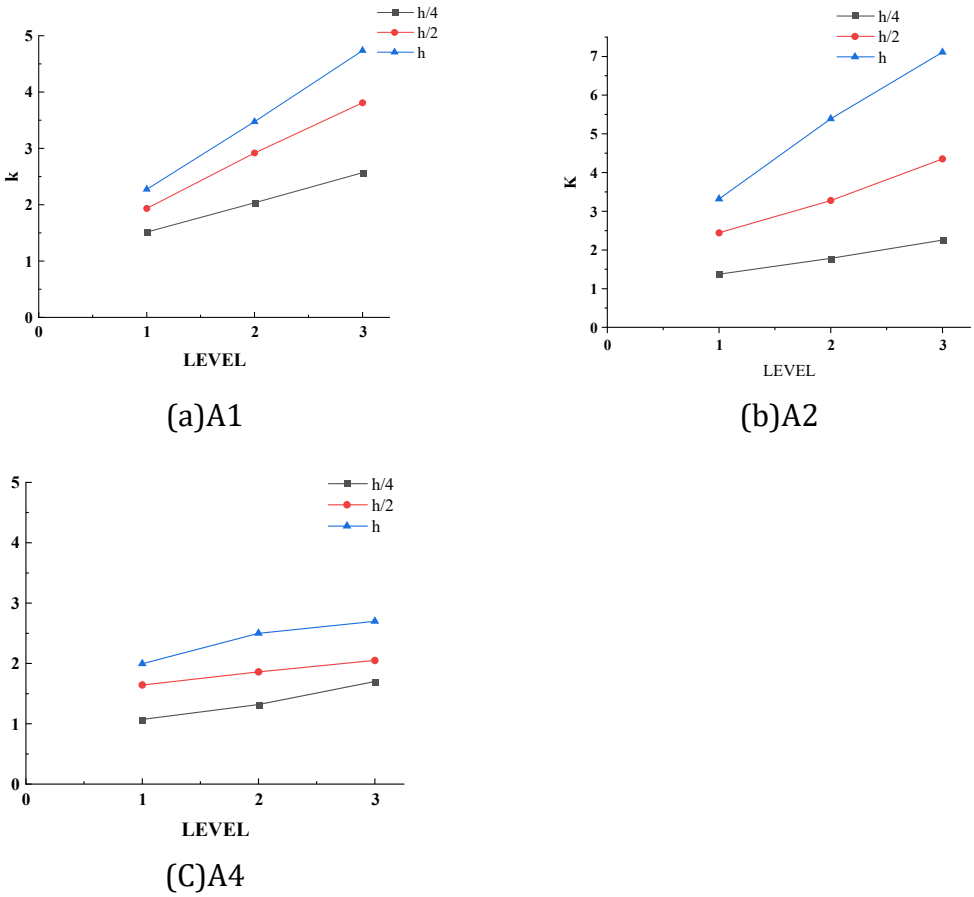

(a)A1 (b)A2

(C)A4

Figure 4. The proportion of different paste layers is increased

It can be seen from Figure 4 that the same ultimate bearing capacity of each specimen is roughly manifested as increasing with the increase of the height and number of layers of the fiber cloth, but under different additive combination structure settings, the number of layers and height of the outer fiber cloth play different roles on the specimen

It can be seen from Table 1 that the ultimate bearing capacity of A1 specimen increases by 0.87%, 2.11% and 2.75% respectively with the increase of the number of layers under 225mm and 450mm under the fiber cloth, and it can be seen from Figure 4 (a) that the increase curve still shows a large upward trend.

The ultimate bearing capacity of A2 and A4 specimens increased by 0.33%, 0.56% and 0.96% respectively with the increase of the number of layers. 0.35%, 0.64%, 0.65%, from Figures4(b) and 4(c) show that the growth trend of the ultimate bearing capacity of different fiber heights slows down.

ISSN: 2472-3703 DOI: 10.6911/WSRJ.202304_9(4).0012

3.4. Typical specimen mises stress cloud

Mises stress cloud diagram of typical specimens A2 and A4 when loading bundles under a single layer of 450mm height paste, carbon fiber cloth, core concrete, steel pipe

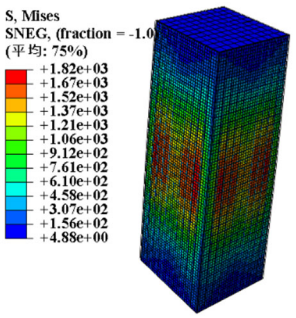

(a)A2 overall

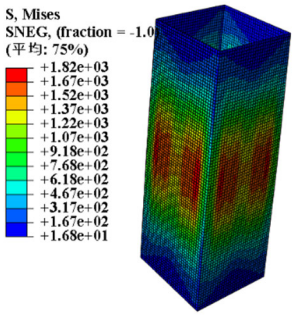

(b)A2 Fiber cloth

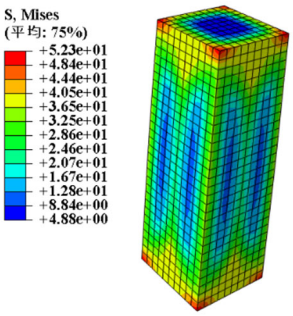

(c)A2 concrete

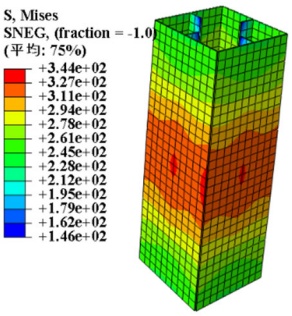

(d)A2 steel tube

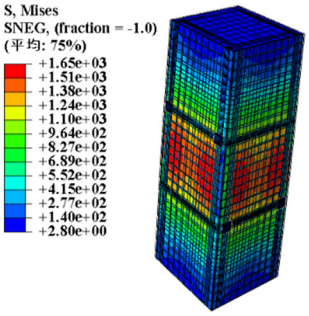

(e)A4 overall

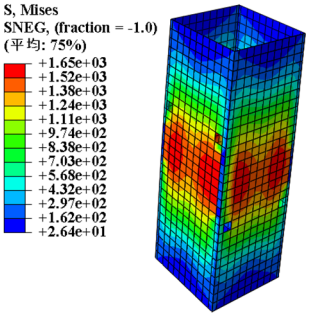

(f)A4 Fiber cloth

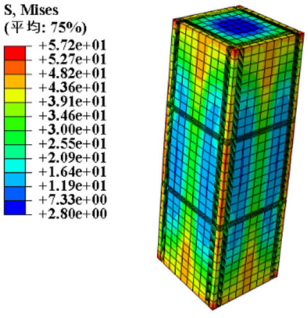

(g)A4 concrete

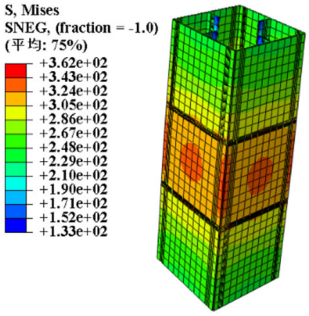

(h)A4 steel tube

Figure 5. MISES cloud diagram of a typical specimen

ISSN: 2472-3703 DOI: 10.6911/WSRJ.202304_9(4).0012

From Fig. 5(b) and Fig. 5(f), it can be seen that the fiber cloth is subjected to greater mises stress, but does not reach the failure strength; The concrete showed that the utilization effect of half-wave drum steel along the stiffener was better, and the maximum force of constraint was close to the corner, which was caused by the constraint mechanism of square steel pipe on concrete. In summary, it shows that setting carbon fiber cloth can improve the integrity of the specimen.

4. CONCLUSION

In this paper, the finite element analysis software is used to carry out numerical simulation of the new composite steel tube concrete structure reinforced by carbon fiber cloth, and the following results are obtained

(1) The use of finite element analysis software can make better analysis convenience for changing the model under a single parameter, and improve the cycle of prediction of urgent problems in engineering.

(2) The external pasted carbon fiber cloth has the greatest improvement in the mechanical properties of steel tube concrete columns under normal circumstances, and the test pieces that have been set up with stiffener combination structure still have better force performance in the later stage of the bearing capacity of the test piece.

REFERENCES

[1] ZHONG S T. APPLICATION AND DEVELOPMENT IN CHINA OF CONCRETE FILLED STEEL TUBULAR STRUCTURE [J]. Architecture Technology, 2001(02):80-82.

[2] HE Z Q.CAI J.CHENG X. Investigation of Behavior of Square CFT Stub Columns with Binding Bars Under Axial Loads [J]. Building Structure, ,2006(08):49-53.DOI:10.19701/j.jzjg.2006.08.014.

[3] CAI J,HENG Z Q. Eccentric-loaded behavior of square CFT columns with binding bars [J]. Journal of Building Structures, 2007(04):25-35.DOI:10.14006/j.jzjgxb.2007.04.005.

[4] CHENG H F. Constitutive equations for civil engineering materials (Volume I Resiliency and modeling) [M].Wu Han: Huazhong University of Science and Technology Pres.240-260.

[5] LI P J, WANG L B. Experimental Study on Eccentric Compression of ribbed Steel-concrete Hollow Columns [J] .Construction Technology,2018,47(19):137-140.